Kutateladze, S. S., et al., "Hydraulic resistance and heat transfer in stabilized flow of non-Newtonian fluids." *Heat transfer—Soviet Research* 2(6), 114 (1970).
Lyon, R. N., "Liquid metal heat transfer coefficients," *Chem. Eng. Progr. Symp. Ser. No. 2*, **47**, 75 (1951).
McComas, S. T., and E. R. G. Eckert, "Combined free and forced convection in a horizontal circular tube," *Trans. Am. Soc. Mech. Engrs., J. Heat Transfer, Ser. C*, **88**, 147 (1966).
McKillop, A. A., "Heat transfer for laminar flow of non-Newtonian fluids in entrance region of a tube," *Intern. J. Heat Mass Transfer*, **7**, 853 (1964).
Matsuhisa, S., and R. B. Bird, "Analytical and numerical solutions for laminar flow of the non-Newtonian Ellis fluid," *AIChE J.*, **11**, 588 (1965).
Michiyoshi, I., "Heat transfer of slurry flow with internal heat generation," Bull. Jap. Soc. Mech. Engrs., **5**, 315 (1962).
Michiyoshi, I., and R. Matsumoto, "Heat transfer of slurry flow with internal heat generation," *ibid.*, **7**, 376 (1964).
———., and M. Hozumi, "Heat transfer of slurry flow with heat generation," *ibid.*, **6**, 496 (1963).
Mitsuishi, N., and O. Miyatake, "Laminar heat transfer to non-Newtonian Ellis model fluids in cylindrical tubes," *Chem. Eng. Japan*, **5**, 82 (1967).
———., "Heat transfer of non-Newtonian laminar flow in tubes with constant wall heat flux," *Kagaku Kogaku*, **32**, 1222 (1968).
———., "Heat transfer with non-Newtonian laminar flow in a tube having a constant wall heat flux," *Intern. Chem. Eng.*, **9**, 352 (1969).
Mizushina, T., et al., "Laminar heat transfer to non-Newtonian fluids in a circular tube (constant heat flux)," *Kagaku Kogaku*, **31**, 250 (1967).
Mori, Y., and K. Futagami, "Forced convective heat transfer in uniformly heated horizontal tubes," 2nd Report, theoretical study, *Intern. J. Heat Mass Transfer*, **10**, 1801 (1967).
Mori, Y., et al., "Forced convective heat transfer in uniformly heated horizontal tubes, 1st report—experimental study on the effect of buoyancy," *ibid.*, **9**, 453 (1966).
Morton, B. R., "Laminar convection in uniformly heated horizontal pipes at low Rayleigh numbers," *Quarterly J. Mech. Appl. Math.*, **12**, 410 (1959).
Newell, P. H., and A. E. Bergles, "Analysis of combined free and forced convection for fully developed laminar flow in horizontal tubes," *Trans. Am. Soc. Mech. Engrs., J. Heat Transfer, Ser. C*, **92**, 83 (1970).
Oliver, D. R., and V. G. Jenson, "Heat transfer to pseudoplastic fluids in laminar flow in horizontal tubes," *Chem. Eng. Sci.*, **19**, 115 (1964).
Petukhov, B. S., and A. F. Polyakov, "Experimental investigation of heat transfer during viscous gravitational flow of liquid in horizontal pipe," *Teplofizika Vysokikh Temp.*, **5**:87 (1967).
———., "Effect of free convection on heat transfer during forced flow in a horizontal pipe," *Teplofizika Vysokikh Temp.*, **5**, 384 (1967).
Pigford, R. L., "Nonisothermal flow and heat transfer inside vertical tubes," *Chem. Eng. Progr. Symp., Ser. No. 17*, **51**, 79 (1955).
Schenk, J., and J. Van Laar, "Heat transfer in non-Newtonian laminar flow in tubes," *Appl. Scientific Research, Sec. A*, **7**, 449 (1958).
Sellars, J. R., M. Tribus, and S. J. Klein, "Heat transfer to laminar flow in a round tube or flat conduit—the Graetz problem extended," *Trans. Am. Soc. Mech. Engrs.*, **78**, 441 (1956).
Sestak, J., and M. E. Charles, "Limiting values of Nusselt number for heat transfer to pipeline flow of non-Newtonian fluids with arbitrary internal heat generation," *Chem. Eng. Progr. Symp. Ser. No. 82*, **64**, 212 (1968).
Shannon, R. L., and C. A. Depew, "Combined forced and free laminar convection in horizontal tube with uniform heat flux," *Trans. Am. Soc. Mech. Engrs., J. Heat Transfer, Ser. C*, **90**, 353 (1968).
———., "Forced laminar flow convection in a horizontal tube with variable viscosity and free-convection effects," *ibid.*, **91**, 251 (1969).
Siegel, R., E. M. Sparrow, and T. M. Hallman, "Steady laminar heat transfer in a circular tube with prescribed wall heat flux," *Appl. Scientific Research, Sec. A*, **7**, 386 (1958).
Siegwarth, D. P., and T. J. Hanratty, "Computational and experimental study of the effect of secondary flow on the temperature field and primary flow in a heated horizontal tube," *Intern. J. Heat Mass Transfer*, **13**, 27 (1970).
Siegwarth, D. P., et al., "Effect of secondary flow on the temperature field and primary flow in a heated horizontal tube," *Intern. J. Heat Mass Transfer*, **12**, 1535 (1969).
Skelland, A. H. P., *Non-Newtonian Flow and Heat Transfer*, Wiley, New York (1967).
Test, F. L., "Laminar flow heat transfer and fluid flow for liquids with temperature dependent viscosity," *Trans. Am. Soc. Mech. Engrs., J. Heat Transfer, Ser. C*, **90**, 385 (1968).
Van Wazer, J. R., et al., *Viscosity and Flow Measurements: A Laboratory Handbook of Rheology*, Interscience, New York (1963).
Yang, K. T., "Laminar forced convection of liquids in tubes with variable viscosity," *Trans. Am. Soc. Mech. Engrs., J. Heat Transfer, Ser. C*, **84**, 353 (1962).

Manuscript received August 27, 1974; revision received and accepted February 3, 1975.

Trickle-Bed Reactor Performance

Part I. Holdup and Mass Transfer Effects

Liquid holdup and mass transfer rates were measured in a 2.58-cm I.D. tube, packed with glass beads and granular CuO · ZnO catalyst or β-naphthol particles, and operated as a trickle bed. Gas-to-liquid (water) transport coefficients were determined from absorption and desorption experiments with oxygen at 25°C and 1 atm. Liquid-to-particle mass transfer was studied using β-naphthol particles.

Holdup and both mass transfer coefficients were unaffected by gas flow rate but increased with liquid rate. The data were correlated with equations that could be used for predicting mass transfer coefficients at high temperatures and pressures for use in the reaction studies reported in Part II.

SHIGEO GOTO and J. M. SMITH
Department of Chemical Engineering
University of California
Davis, California 95616

Correspondence concerning this paper should be addressed to J. M. Smith. S. Goto is on leave from University of Nagoya, Japan.

SCOPE

Oxidation of organic pollutants in water with a solid catalyst offers some potential as an alternative process for water purification. Catalysts developed up to this time, which are usually metal oxides, require temperatures of about 200°C. This means that the reactor must be operated under pressure in order to maintain the water in the liquid phase. Further, inadequate oxygen for complete reaction can be dissolved in the water. Hence catalytic oxidation of pollutants in water is well suited for trickle-bed reactor operation where a continuous supply of oxygen is introduced with the gas (air) stream. The two parts of the paper describe studies in a laboratory-scale trickle-bed reactor for oxidation of formic acid in water at 40 atm pressure and 212° to 240°C. The purpose of the work is to develop data and procedures useful for design of this type of reactor system.

The design approach for a trickle-bed reactor may be divided into two aspects. The first is a procedure to predict the global rate, that is, the rate associated with a single catalyst particle. Evaluation of this rate requires intrinsic kinetics, intraparticle diffusion, and mass transfer rates between gas, liquid, and solid (catalyst) phases. The second aspect is a model to predict the conversion in the reactor as a whole. Such models must describe the nature of the mixing in the gas and liquid streams; that is, plug flow, flow with axial dispersion, etc. It is here that liquid holdup is involved. In the work reported, experimental and predicted results were obtained for both aspects.

In Part I, holdup, and gas-to-liquid and liquid-to-solid mass transfer rates are presented for a trickle-bed apparatus of the same characteristics as used in Part II for the reaction studies. Of necessity these measurements were at 1 atm and room temperature. Correlations were suggested for predicting the mass transfer rates at high temperatures and pressures.

Two types of data are given in Part II: global rates measured in a differential reactor with low conversions of formic acid and oxygen, and high-conversion (60 to 97% for formic acid) results obtained with deeper catalyst beds in the same reactor. The global rates were compared with predicted values using known intrinsic kinetics and the mass transfer coefficients reported in Part I. The integral reactor data were compared with predictions based upon plug-flow and axial dispersion models.

CONCLUSIONS AND SIGNIFICANCE

Most correlations for dynamic holdup and interphase mass transport are based upon data obtained in absorption towers using special types of relatively large particles (that is, Raschig rings, Berl saddles, etc.). However, Satterfield and Way (1972) reported holdup data for small glass beads and for extruded catalyst particles. Our holdup data did not agree with the correlations based upon the absorption tower data, except for the largest particles studied in our work (0.41-cm glass beads). The correlating procedure of Satterfield and Way fit well our data for the smaller particles but not that for 0.41-cm glass beads. Apparently the effect of particle size on holdup changes at a particle size from 0.3 to 0.4 cm.

For the oxygen transport system we found the mass transfer resistance from bulk gas to gas-liquid interface to be negligible. On the liquid side of this interface, the correlating procedure for the mass transfer coefficient k_La of Sherwood and Holloway (1940) fit our data well. This correlation is in terms of parameters characteristic of packing size and shape. Experimental results for the mass transfer coefficient k_sa from liquid to outer particle surface did not agree with the correlation proposed by Van Krevelen and Krekels (1948) for trickle beds, possibly because their correlation was based upon data for larger particle sizes. An equation analogous to that of Sherwood and Holloway was developed for use in predicting k_sa at reaction conditions.

Holdup and all mass transfer coefficients were unaffected by gas flow rate at the conditions of our experiments.

Accurate calculations of global reaction rates from the measured mass transfer results was somewhat hindered by lack of experimental data for diffusivities of oxygen and formic acid in water at 212° to 240°C and 40 atm pressure. Predicted global rates were from 0 to 35% higher than the measured rates. Gas flow rate did not influence the global rate. Increases in liquid flow rate and in temperature increased the global rate, indicating that mass transfer and intrinsic kinetics were both important factors in reactor performance.

Integral reactor conversions of formic acid were calculated from intrinsic kinetics, effective intraparticle diffusivities, k_sa, and k_La as determined from the data given in Part I. Agreement between predicted and experimental results was within 10%. Plug flow of both gas and liquid streams gave conversions 1 to 2% higher than when axial dispersion was accounted for in the liquid phase. This difference was less than the effects of intraparticle diffusion, k_sa, and of k_La on the conversion. The retardation of the rate and conversion due to gas-to-liquid mass transfer was the most important transport effect, followed by intraparticle diffusion, even for catalyst particles of 0.0541 cm diameter. The relatively great significance of gas-to-liquid transport with respect to axial dispersion means that reactor modeling questions, such as holdup and residence time distribution, were much less important than accurate values for mass transport coefficients.

The most common arrangement for a trickle-bed reactor is concurrent downflow of liquid and gas over a fixed bed of catalyst particles and such a configuration was used in this work. In the reaction studies (Part II) one reactant was introduced with the gas stream and the other with the liquid. Hence, the global reaction rate at any axial position in the reactor may be retarded by gas-to-liquid and liquid-to-particle mass transfer. Also the conversion of the reactant in the liquid is dependent upon the residence time, which in turn is determined in part by the liquid holdup. Design of trickle-bed reactors should include the effects of these factors, yet there is inadequate information available for both mass transfer rates and for holdup, particularly for small diameter particles and for low liquid flow rates.

The objective in Part I was to obtain holdup and mass

Table 1. Static Holdup and Bed Properties

	d_p, cm	ρ_p, g/cm³	ρ_s, g/cm³	ϵ_p	ϵ_B	a_t*, cm²/cm³	H_s	H_{is}	H_{es}
Glass beads	0.413	2.15	2.15	0.0	0.371	9.14	0.0282	0.0	0.0282
CuO · ZnO Catalyst	0.291	2.35	5.29	0.56	0.441	11.5	0.371	0.313	0.058
CuO · ZnO Catalyst	0.0541	2.35	5.29	0.56	0.453	60.7	0.429	0.306	0.123
β-naphthol	0.241	1.17	1.22	0.038	0.483	12.9	—	—	—
β-naphthol	0.0541	1.17	1.22	0.038	0.520	53.2	—	—	—

* Calculated by assuming that the particles have a spherical diameter of d_p; that is, $a_t = \frac{6(1-\epsilon_B)}{d_p}$.

transfer data for both porous and nonporous particles. Measurements were made at 25°C and atmospheric pressure using water for the holdup studies, absorption and desorption of oxygen for the gas-to-fluid mass transfer, and dissolution of β-naphthol for particle-to-fluid mass transfer.

LIQUID HOLDUP

The residence time of liquid in a trickle-bed reactor is determined by the dynamic holdup H_d, which is the volume of liquid that drains from the bed, after gas and liquid flows are stopped, divided by the total volume of the bed. In addition to H_d, static holdups were also determined. The total static holdup H_s is the volume fraction of liquid that remains after draining the bed. H_s was evaluated by weighing the bed after H_d had been determined and comparing this weight with that of the dry bed. For porous particles the static holdup consists of the liquid in the intraparticle pores H_{is} and the liquid held in the interparticle space H_{es}. If the internal pores are completely filled with liquid, H_{is} is calculable from the bed and particle void fractions according to the equation

$$H_{is} = \epsilon_p(1 - \epsilon_B) \qquad (1)$$

Then H_{es} is obtained by subtracting H_{is} from H_s.

The same apparatus (Figure 1) was used for holdup and mass transfer studies. The particles were held in a glass tube (I.D. = 2.58 cm, packed bed length = 15.2 cm) by a stainless steel screen. The liquid entered the top of the bed through a liquid distributor containing five capillary tubes (0.1 cm I.D., 0.5 cm long). Preliminary

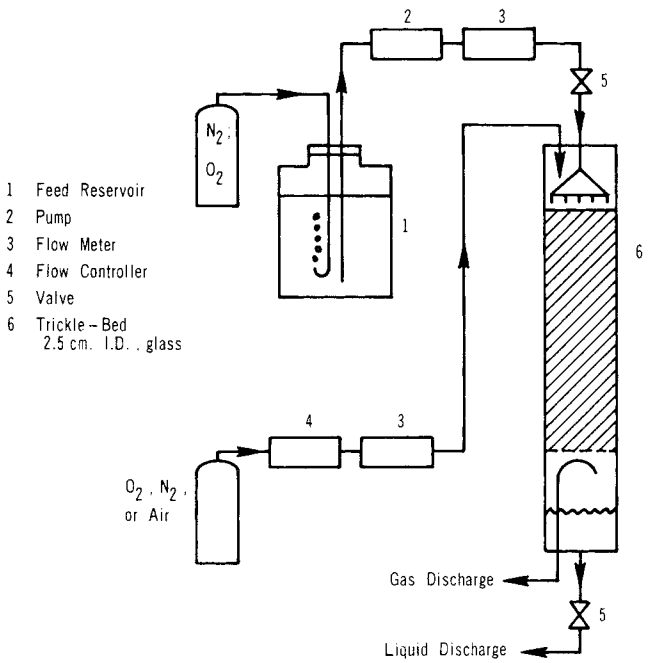

Fig. 1. Apparatus for holdup and mass transfer data.

experiments showed that a 0.5-cm length of capillary provided enough flow resistance to ensure nearly equal flow of liquid from each tube. The five tubes were located vertically in the cross section of the glass tube so that the flux of liquid was approximately uniform.

Data were obtained for glass beads, porous, CuO · ZnO catalyst particles (Chemetron Corp. G-66B) and for nonporous, granular β-naphthol particles. The catalyst particles were the same as those employed for the reaction studies (Part II). Properties of the several particles and the beds are given in Table 1. The original ¼ in. × ⅛ in. cylindrical catalyst pellets were cut into equal pie-shaped quarters which had an equivalent spherical diameter $d_p = 6V_p/S_p$ of 0.291 cm. For the smaller size, the pellets were crushed and sieved, retaining the 28-32 mesh fraction (average d_p = 0.0541 cm). The β-naphthol particles were crushed pellets with size ranges of 28-32 and 7-9 mesh (average d_p = 0.241 cm).

For dynamic holdup measurements the inlet and outlet valves [Figure 1(5)] were simultaneously closed after steady state conditions were achieved. Then the volume of liquid that would drain from the column was measured. After a maximum period of 30 min., the drainage essentially ceased. In the range of gas rates from 0 to 4.0 cm³/s (25°C, 1 atm), H_d was nearly constant for a fixed liquid rate. A maximum variation of 6% in H_d with F_g was observed for the 0.291-cm catalyst particles.

The static holdups are listed in Table 1. It was not possible to measure static values for β-naphthol because the weight of the particles changed due to dissolution. The measured dynamic holdups are shown by the data points in Figure 2.

The most frequently cited correlation for dynamic holdup is that of Otake and Okada (1953) which is based upon data obtained in absorption columns packed with nonporous particles of diameters from 1 to 5 cm. They proposed the following correlations:

1. For spheres ($10 < Re < 2000$):

$$H_d = 1.25(Re)^{0.676}\,(Ga)^{-0.44}\,a_t d_p \qquad (2)$$

2. For Rasching rings and broken solids:

$$H_d = 15.1\,(Re)^{0.676}\,(Ga)^{-0.44}\,(a_t d_p)^{-0.60}; \qquad 10 < Re < 2000 \qquad (3)$$

$$H_d = 21.1\,(Re)^{0.51}\,(Ga)^{-0.44}\,(a_t d_p)^{-0.60}; \qquad 0.01 < Re < 10 \qquad (4)$$

where a_t is the total external surface area of the particles per unit volume of the bed (see Table 1).

The dotted lines in Figure 2 represent Equation (2) for the glass beads, and Equations (3) and (4) for the granular catalyst and β-naphthol particles. Only for the relatively large glass beads do these correlations fit the data. The deviations increase with decrease in particle size. The solid lines represent Equation (5), as discussed in the following paragraph.

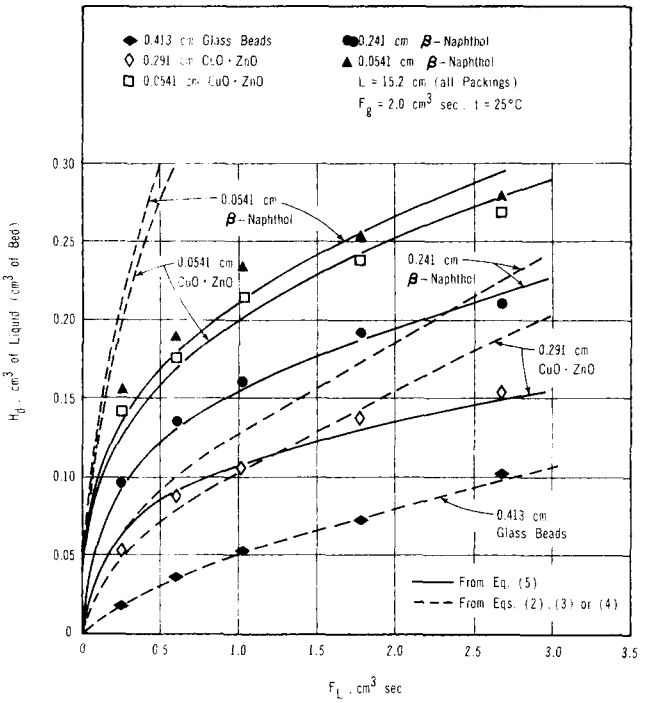

Fig. 2. Effect of liquid flow rate on dynamic holdup.

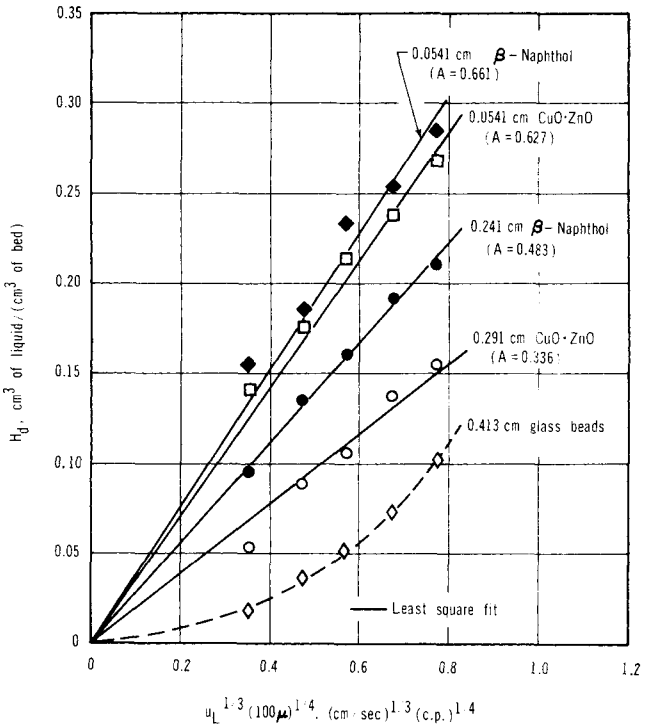

Fig. 3. Dynamic holdup vs. $u_L^{1/3}(100\mu)^{1/4}$.

Satterfield and Way (1972) proposed that the dynamic holdup in a trickle-bed reactor was a function of the superficial velocity and viscosity of the liquid:

$$H_d = A(u_L)^{1/3}\,(100\mu)^{1/4} \qquad (5)$$

with the dimensional parameter A to be determined from holdup data for each type of particle. Equation (5) was based upon data for 0.3-cm glass beads and 0.16 and 0.32-cm cylinders of SiO_2-Al_2O_3 catalyst. Our data are plotted according to Equation (5) in Figure 3. This method of correlations appears to be adequate for the porous or solid particles so long as d_p is less than 0.3 to 0.4 cm. However, the deviation from a linear relationship is significant for 0.4-cm glass beads. The solid lines in Figure 3 represent Equation (5) with the indicated values of A.

It is concluded from these comparisons with holdup data that for downflow trickle-bed reactors the effect of particle size on H_d changes at a d_p of 0.3 to 0.4 cm. Existing correlations for H_d should be used with caution for d_p values beyond the range of data upon which the correlations are based. Figures 2 and 3 show that the holdup for the nonporous β-naphthol is slightly higher than for porous CuO · ZnO particles of the same particle size. This difference is due primarily to the larger bed porosity (ϵ_B, Table 1) for the β-naphthol case rather than due to differences in surface characteristics. It should be noted that the packed bed depth and the ratio of tube-to-particle diameter were both relatively low for all the holdup measurements.

GAS-TO-LIQUID MASS TRANSFER

Since the application of mass transfer data in Part II is for an oxidation process, the transport of oxygen between the gas and liquid phase in a trickle bed was studied. For such a slightly soluble gas the interphase transport is expected to be controlled by the liquid phase resistance and our results substantiated this conclusion.

The absorption measurements were made by feeding oxygen-free, distilled water and pure oxygen gas to the bed using the apparatus shown in Figure 1. The water was stripped of oxygen with a stream of nitrogen prior to making a run. For desorption measurements, the distilled water was first saturated with pure oxygen and the gas stream consisted of pure nitrogen.

The oxygen concentration C_{L,O_2} in the water was measured by stripping a sample with helium in a packed column and passing the exit gases to a chromatograph for analysis. Details of the procedure have been reported (Baldi et al., 1974). Oxygen was determined in the feed and discharge water streams for runs with different liquid and gas flow rates. The oxygen concentration in the discharge stream was nearly independent of gas flow rate over the range 1.0 to 4.0 cm³/s. For the bed of 0.291-cm CuO · ZnO particles C_{L,O_2} varied by 4% at a liquid flow rate of 1.03 cm³/s. This indicates that the effect of F_g on the mass transfer coefficient k_L was insignificant. The variation in C_{L,O_2} with liquid flow rate is illustrated in Figure 4 for desorption runs with the column packed with

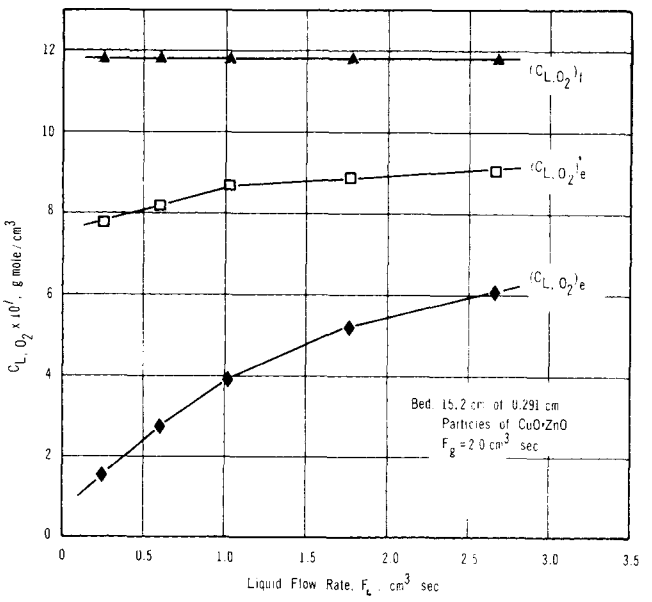

Fig. 4. Concentrations of oxygen in desorption runs.

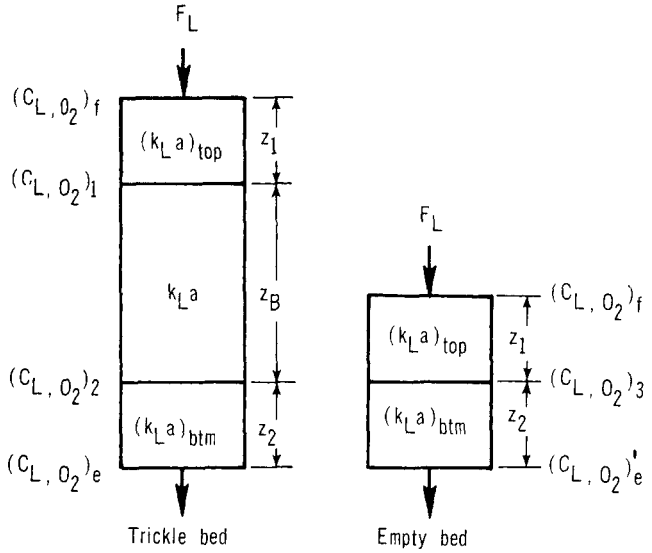

Fig. 5. Modeling of end effects in trickle-bed reactor.

0.291-cm CuO · ZnO particles. To test for mass transfer in the end regions, between liquid distributor and top of bed and between bottom of bed and liquid level in the tube, C_{L,O_2} was measured in the discharge stream when the packing was removed and the liquid distributor was lowered to just above the screen. This concentration, designated $(C_{L,O_2})_e'$, was 24 to 36% less than $(C_{L,O_2})_f$, indicating that considerable mass transport was occurring in the end regions of the bed. Figure 4 shows $(C_{L,O_2})_e'$ for one bed.

To determine k_La for the bed itself, the mass transfer at the top $(k_La)_{top}$ and bottom $(k_La)_{btm}$ end regions was accounted for by the procedure depicted in Figure 5. If axial dispersion is neglected, mass balances for oxygen in the two end regions and the bed itself, for the desorption case, may be written

$$F_L\,dC_{L,O_2} = -\,(k_La)_{top}\,(C_{L,O_2} - 0)S\,dz \qquad (6)$$

$$F_L\,dC_{L,O_2} = -\,(k_La)\,(C_{L,O_2} - 0)S\,dz \qquad (7)$$

$$F_L\,dC_{L,O_2} = -\,(k_La)_{btm}\,(C_{L,O_2} - 0)S\,dz \qquad (8)$$

At the gas rates used the concentration of oxygen in the gas was negligible. Boundary conditions for these equations are

$$C_{L,O_2} = (C_{L,O_2})_f \quad \text{at} \quad z = 0 \qquad (9)$$

$$= (C_{L,O_2})_1 \quad \text{at} \quad z = z_1 \qquad (10)$$

$$= (C_{L,O_2})_2 \quad \text{at} \quad z = z_1 + z_B \qquad (11)$$

$$= (C_{L,O_2})_e \quad \text{at} \quad z = z_1 + z_B + z_2 \qquad (12)$$

where z_1, z_B, and z_2 are the lengths of the upper end section, bed, and lower end section, as shown in Figure 5. If Equations (6) to (8) are solved with the boundary conditions, and the concentrations $(C_{L,O_2})_1$ and $(C_{L,O_2})_2$ are eliminated from the three integrated equations, an expression involving only $(C_{L,O_2})_f$ and $(C_{L,O_2})_e$ is obtained:

$$(C_{L,O_2})_e = (C_{L,O_2})_f \exp\left[\frac{-(k_La)_{top}\,z_1 - (k_La)z_B - (k_La)_{btm}\,z_2}{F_L/S}\right] \qquad (13)$$

In a similar way the expression for the exit concentration in the empty bed is

$$(C_{L,O_2})_e' = (C_{L,O_2})_f \exp\left[\frac{-(k_La)_{top}\,z_1 - (k_La)_{btm}\,z_2}{F_L/S}\right] \qquad (14)$$

Dividing Equation (13) by (14) gives the following expression for k_La for the bed in terms of the measured concentrations $(C_{L,O_2})_e$ and $(C_{L,O_2})_e'$:

$$k_La = \frac{F_L/S}{z_B} \ln\left[\frac{(C_{L,O_2})_e'}{(C_{L,O_2})_e}\right] \qquad (15)$$

A similar derivation for the absorption case yields

$$k_La = \frac{F_L/S}{z_B} \ln\left[\frac{C^*_{L,O_2} - (C_{L,O_2})_e'}{C^*_{L,O_2} - (C_{L,O_2})_e}\right] \qquad (16)$$

where C^*_{L,O_2} is the concentration of oxygen in water in equilibrium with pure oxygen gas. For 1 atm and 25°C this value is 12.6×10^{-7} g mole/cm³ (Perry, 1963).

The effect of axial dispersion was evaluated by estimating a dispersion coefficient E from the correlation of Furzer and Michell (1970) which is based on data for countercurrent, two-phase flow in a packed bed. Solution of the mass balances using such dispersion coefficients gave k_La values no more than 3% higher than when axial dispersion is neglected. This small increase justifies neglecting axial dispersion in the analysis of the mass transfer data. For k_sa (see next section) the bed depth was less so that the axial dispersion effect was larger, but less than 10%. In terms of the overall effect of mass transfer on the trickle-bed reactor performance discussed in Part II, k_La is several times as important as k_sa.

Values of k_La determined from Equations (15) and (16) are shown in Figure 6 for beds of glass beads and of catalyst particles. Absorption and desorption results for the glass beads agree well with each other. This is evidence that the interphase mass transfer is controlled by the resistance in the liquid phase since in one case the oxygen mole fraction in the gas is nearly 100% and in the other case it is low. In view of this agreement, only the more accurate desorption measurements were made for the catalyst particles.

Based upon a study of desorption of O_2, H_2, and CO_2 from water in countercurrent packed beds, Sherwood and Holloway (1940) found also that k_La was independent of gas flow rate. Their dimensional correlation is

$$\frac{k_La}{D} = \alpha_L \left(\frac{G_L}{\mu}\right)^{n_L} \left(\frac{\mu}{\rho D}\right)^{1/2} \qquad (17)$$

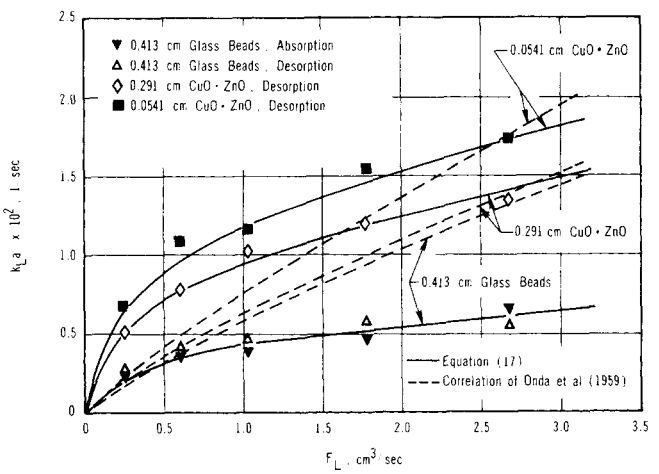

Fig. 6. Effect of liquid flow rate on k_La (F_g = 2.0 cm³/s; z_B = 15.2 cm).

where the proper units are those shown in the Notation, and n_L and α_L are related to the mass transfer surface and geometry of the particles and are specific for each bed. This form of correlation for k_La agreed well with our data as indicated by the straight lines obtained in Figure 7 where $(k_La/D)/(\mu/\rho D)^{1/2}$ is plotted versus G_L/μ. The solid curves in Figure 6 represent Equation (17) with the following values of α_L and n_L:

Particles	α_L, $(\text{cm})^{n_L-2}$	n_L
Glass beads (0.413 cm)	2.8	0.40
CuO · ZnO (0.291 cm)	6.0	0.41
CuO · ZnO (0.0541 cm)	7.8	0.39

The dimensionless correlation of Onda et al. (1959) for k_La for absorption columns packed specifically with Raschig rings does not agree with our data for trickle beds containing glass beads or granular particles. The effect of liquid rate on k_La predicted from this correlation is greater than observed experimentally, as shown by the dotted lines in Figure 6. The data in Figure 6 will be used in Part II for calculating the gas-to-liquid mass transfer resistance under reaction conditions.

LIQUID-TO-PARTICLE MASS TRANSFER

Mass transfer rates from particle-to-liquid were measured by flowing distilled water (at 25°C and 1 atm) down through short beds of β-naphthol particles. Bed lengths z_B are given in Figure 8. Runs were made with concurrent air flow for trickle-bed operation and with the bed full of liquid (no gas phase). Concentrations of β-naphthol in the liquid were measured using a Beckman DK-2A spectrophotometer at a wavelength of 315 millimicrons where β-naphthol has a large absorptivity. The measured solubility in water at 25°C was 0.0748 g/(100g H_2O) which agrees well with the reported (Perry, 1963) value of 0.074 g/(100g H_2O). End effects were not involved for these runs so that k_sa can be calculated from a mass balance for β-naphthol in the bed. Neglecting axial dispersion, this expression is

$$F_L\, d\,C_{L,N} = (k_sa)\,(C^*_{L,N} - C_{L,N})S\, dz \qquad (18)$$

Integrating with the appropriate boundary conditions and solving for k_sa gives

$$k_sa = \frac{F_L/S}{z_B} \ln\left[\frac{C^*_{L,N} - (C_{L,N})_f}{C^*_{L,N} - (C_{L,N})_e}\right] \qquad (19)$$

Here z_B is the average length of packed bed. Because of dissolution, the length decreases during the run. This decrease was not large, ranging from 1 to 7%.

The values of k_sa evaluated from Equation (19) for trickle-bed operation were nearly insensitive to the gas rate for F_g from 0 to 4.0 cm³/s. For example, k_sa changed by 7% between zero gas flow and 4.0 cm³/s for 0.241-cm particles, at a liquid flow rate of 1.03 cm³/s. Note that even for $F_g = 0$, a gas phase existed in the bed. Hence, the conditions are different than for the liquid-full runs.

The results are displayed in Figure 8 for both trickle-bed and liquid-full conditions. Several correlations have been presented for fluid-particle mass transfer in liquid-full packed beds and these agree, in general, with our data. For example, the dotted curves in Figure 8 represent the correlation of Evans and Gerald (1953). This correlation, which permits calculation of k_s, may be written

$$\frac{k_s}{u_L}\left(\frac{\mu}{\rho D}\right)^{2/3} = 1.48(Re)^{-0.52} \qquad (20)$$

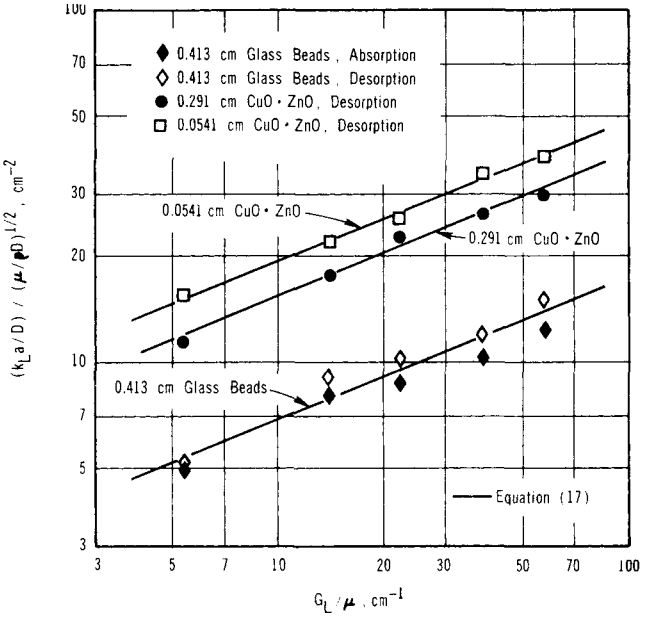

Fig. 7. Correlation of k_La.

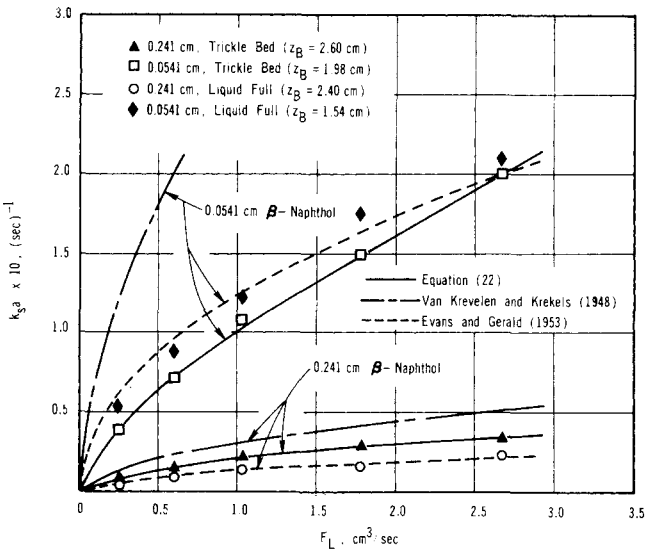

Fig. 8. Effect of liquid flow rate on k_sa (F_g = 2.0 cm³/s).

The effective mass transfer surface used to obtain the product k_sa is based upon the total external surface of the particles per unit volume of bed; that is, $a = a_t = 6(1 - \epsilon_B)/d_p$.

Figure 8 shows that k_sa is greater in the trickle bed than in the liquid-full bed, at the same flow rate, for the larger particles. This is probably due to the larger linear velocities in trickle beds where part of the volume is occupied by gas. Correlations such as that of Van Krevelen and Krekels (1948) for trickle beds and Evans and Gerald (1953) for liquid-full beds indicate similar results. In contrast, our experimental data for the smaller particles (0.0541 cm) show k_sa to be larger for liquid-full operation. Possibly the entire external surface is not effective for mass transfer in trickle beds containing very small particles. If this effect predominates over the velocity factor, k_sa would be greater for liquid-full operation.

The dot-dash curves in Figure 8 represent the Van Krevelen and Krekels correlation, which may be written

$$\frac{k_s}{Da_t} = 1.8\left(\frac{G_L}{\mu a_t}\right)^{1/2}\left(\frac{\mu}{\rho D}\right)^{1/3} \qquad (21)$$

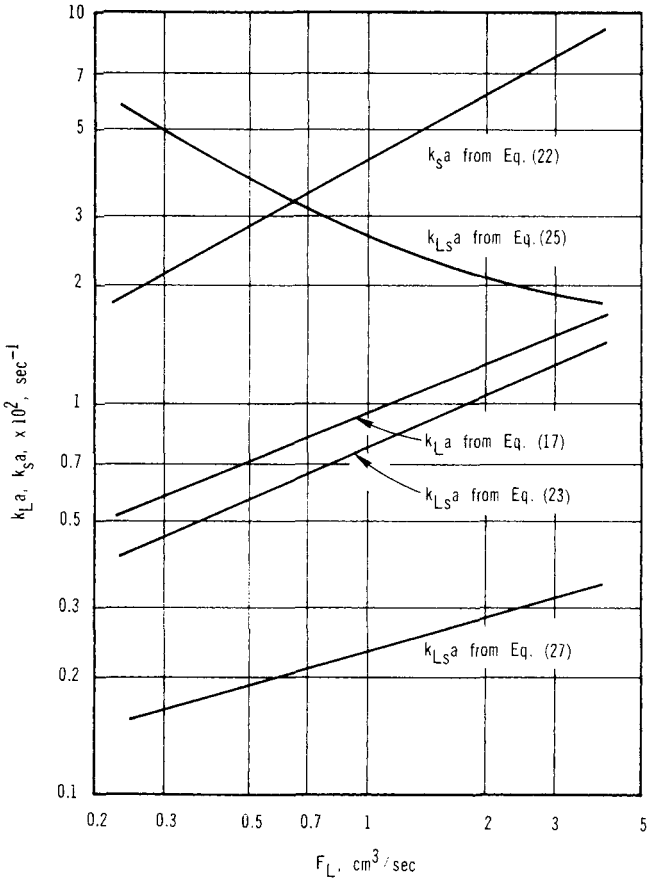

Fig. 9. Overall mass transfer rate in trickle bed (0.291-cm CuO·ZnO particles).

In addition to not predicting the relative values of k_sa for trickle-bed and liquid-full operation for the smaller particles, Equation (21) does not well represent the trickle-bed data for either particle size. The correlation was developed from data for larger (0.29 to 1.4 cm) particles. It is concluded that the effect of particle size on k_sa in trickle beds can change for particles smaller than about 0.2 cm.

In order to obtain a suitable correlation of k_sa for use in Part II, dimensional Equation (17) was modified to the form

$$\frac{k_sa}{D} = \alpha_s \left(\frac{G_L}{\mu}\right)^{n_s} \left(\frac{\mu}{\rho D}\right)^{1/3} \tag{22}$$

where α_s and n_L have values which are specific for a particular particle size and shape and bed packing. Equation (22) agrees well (solid curves in Figure 8) with the experimental data for the following values of α_s and n_s:

β-Naphthol particle sizes, d_p	α_s $(cm)^{n_s-2}$	n_s
0.241	45.	0.56
0.0541	153.	0.67

OVERALL MASS TRANSFER IN A TRICKLE BED

Equations (17) and (22) provide correlations that may be used to predict the overall mass transfer rate from gas to particle for the specific trickle beds used in this work. If the two concentration boundary layers near the gas-liquid and liquid-solid interfaces do not overlap during the flow of liquid over one particle, the overall mass transfer coefficient is given by (Satterfield, 1970)

$$\frac{1}{k_{Ls}a} = \frac{1}{k_La} + \frac{1}{k_sa} \tag{23}$$

Figure (9) shows the curve of $k_{Ls}a$ versus liquid flow rate calculated from Equations (17), (22), and (23) for the transfer of oxygen in a bed of 0.291-cm CuO · ZnO particles. Since k_La is several times smaller than k_sa, the line for the overall coefficient closely parallels that for k_La. In calculating k_sa from Equation (22), the molecular diffusivity of oxygen in water was used. The diffusivities of oxygen and β-naphthol at 25°C were estimated to be 2.26×10^{-5} cm^2/s and 0.774×10^{-5}, respectively, from the Othmer and Thaker equation (Reid and Sherwood, 1966). The values of α_s and n_s determined for the 0.241-cm particles of β-naphthol were assumed to apply even though the particle size was somewhat less than the 0.291 cm for the CuO · ZnO particles.

Experimental values of k_La and k_sa are necessary for predicting the overall coefficient. For example, in the absence of such information, it has been proposed (Satterfield and Way, 1972) that $k_{Ls}a$ could be calculated from the dynamic holdup using the expression

$$k_{Ls} = \frac{D}{H_d/a_t} \tag{24}$$

or

$$(k_{Ls}a) = \frac{D\,a_t^2}{H_d} \tag{25}$$

Equation (25) is based upon two assumptions: complete wetting of the particles so that the total external surface a_t may be employed, and molecular diffusion through a film of thickness H_d/a_t. The values of $k_{Ls}a$ calculated from Equation (25) using the H_d data in Figure 2 for 0.291-cm particles of CuO · ZnO are also shown in Figure 9. This curve is higher than that based upon the experimentally determined coefficients [Equation (23)] and shows a different trend with liquid flow rate. This is significant since the curve based upon Equation (25) is sometimes used as a conservative estimate for $k_{Ls}a$. On the basis that the error in this estimation method is due to a_t not representing the effective interfacial area, a_t in Equation (25) can be replaced with a_w. The relation between a_w and a_t for 0.291-cm granular particles is not known. However, we can approximate this relation by employing the correlation cited by Onda et al. (1959) for a_w for columns packed with Raschig rings:

$$\frac{a_w}{a_t} = 1 - 1.02 \exp\left[-0.278 \left(\frac{G_L}{a_t\,\mu}\right)^{0.4}\right] \tag{26}$$

Using this expression for a_w in the following form of Equation (25)

$$(k_{Ls}a) = \frac{D\,a_w^2}{H_d} \tag{27}$$

gives the lower line in Figure 9. This result shows the same trend with liquid rate as the experimental data [Equation (23)], but the values are much too low. Neither Equation (25) or (27) are reliable for predicting $k_{Ls}a$ for the trickle beds used in our studies.

ACKNOWLEDGMENT

The financial assistance of the Water Resources Center, University of California, Grant W-392, is gratefully acknowledged. The Chemetron Corporation kindly supplied the ZnO·CuO catalyst.

NOTATION

A = parameters in Equation (5), $(cm/s)^{-1/3}(g/cm\,s)^{-1/4}$

a = effective external surface area for mass transfer, $cm^2/(cm^3$ of empty tube)

a_t = total external surface area of particles, $cm^2/(cm^3$ of empty tube)
a_w = wetted external surface area of particles, $cm^2/(cm^3$ of empty tube)
B = $2D_{e,O_2}C_{s,O_2}/D_{e,FA}C_{s,FA}$
C = concentration, g-mole/cm^3
C_L^* = concentration in liquid in equilibrium with gas, g-mole/cm^3
D = molecular diffusivity in liquid, cm^2/s
D_e = effective intraparticle diffusivity, cm^2/s
d_p = particle diameter, cm
E = axial dispersion coefficient, cm^2/s
E_f = effectiveness factor of catalyst particle
F_g = volumetric flow rate of gas at 1 atm, 25°C, cm^3/s
F_L = volumetric flow rate of liquid at 1 atm, 25°C, cm^3/s
Ga = Gallileo number, $d_p^3\ g\ \rho^2/\mu^2$
G_L = superficial liquid flow rate, $g/(cm^2)s$
g = acceleration of gravity, cm/s^2
H = Henry's Law constant, (cm^3 of liquid)/(cm^3 of gas)
H_d = dynamic holdup, (cm^3 of liquid)/(cm^3 of bed)
H_{es} = external static holdup
H_{is} = internal static holdup
H_s = static holdup
k_L = mass transfer coefficient from gas to liquid, cm/s
k_{Ls} = overall mass transfer coefficient from gas to particle, through a liquid layer, cm/s
k_s = mass transfer coefficient from liquid to particle, cm/s
$k^*_{O_2}$ = intrinsic second-order rate constant for O_2 consumption, $cm^6/(g\ mole)(g)(s)$
$\hat{m}$ = generalized Thiele modulus
n_L = parameter in Equation (17)
n_s = parameter in Equation (22)
P = pressure, atm
Pe = Peclet number, $d_p u_L/E$
R = reaction rate, g-mole/(g)s
Re = Reynolds number, $d_p G_L/\mu$
S = cross sectional area of tube, cm^2 (5.23 cm^2 for glass tube, 5.07 cm^2 for stainless steel reactor)
Sc = Schmidt number, $\mu/\rho D$
S_p = external surface area of particle, cm^2
t = temperature, °C
u_L = superficial velocity of liquid, cm/s
V_p = volume of particle, cm^3
W = mass of catalyst particles, g
x_{FA} = conversion of formic acid in liquid at the exit of the reactor
$Y_{g,O_2} = C_{g,O_2}/(C_{g,O_2})_f = C^*_{L,O_2}/(C^*_{L,O_2})_f$
$Y_{L,O_2} = C_{L,O_2}/(C^*_{L,O_2})_f$
$Y_{s,O_2} = C_{s,O_2}/(C^*_{L,O_2})_f$
$Y_{L,FA} = C_{L,FA}/(C_{L,FA})_f$
$Y_{s,FA} = C_{s,FA}/(C_{L,FA})_f$
z = axial coordinate in reactor tube, cm
z_B = total length of packed bed, cm

Greek Letters

α_L = parameter in Equation (17), $(cm)^{n_L-2}$
α_s = parameter in Equation (22), $(cm)^{n_s-2}$
ϵ_B = void friction in the bed
ϵ_p = porosity in the particle
ρ = density of water, g/cm^3
ρ_B = bulk density of particles in bed, g/cm^3
ρ_p = apparent density of particle, g/cm^3
ρ_s = solid-phase density of particle, g/cm^3
μ = fluid viscosity, g/cm s

Subscripts

e = exit
f = feed
FA = formic acid
g = gas phase
L = liquid phase
N = β-naphthol
S = external surface of catalyst

LITERATURE CITED

Baldi, G., S. Goto, C. K. Chow, and J. M. Smith, "Catalytic Oxidation of Formic Acid in Water," *Ind. Chem. Eng. Process Design Develop*, **13**, 447 (1974).

Bischoff, K. B., "Effectiveness Factors for General Reaction Rate Forms," *AIChE J.*, **11**, 351 (1965).

Evans, G. C., and C. F. Gerald, "Mass Transfer from Benzoic Acid Granules to Water in Fixed and Fluidized Beds at Low Reynolds Numbers," *Chem. Eng. Progr.*, **49**(3), 135 (1953).

Furzer, I. A., and R. W. Michell, "Liquid-Phase Dispersion in Packed Beds with Two-Phase Flow," *AIChE J.*, **16**, 380 (1970).

Hartman, M., and R. W. Coughlin, "Oxidation of SO_2 in a Trickle-Bed Reactor Packed with Carbon," *Chem. Eng. Sci.*, **27**, 867 (1972).

Himmelblau, D. M., "Solubility of Inert Gases in Water, 0°C to near the Critical Point of Water," *J. Chem. Eng. Data*, **5**, 10 (1960).

Hoog, H., H. G. Klinkert, and A. Schaafsma, "New Shell Hydrodesulfurization Process Shows these Features, "*Petroleum Refiner*, **32**, 137 (1953).

Hougen, O. A., and K. M. Watson, *Chemical Process Principles*, Part III, p. 873, Wiley, New York (1947).

Onda, K., E. Sada, and Y. Murase, "Liquid-Side Mass Transfer Coefficients in Packed Towers," *AIChE J.*, **5**, 235 (1959).

Otake, T., and K. Okada, "Liquid Holdup in Packed Towers," *Kaguku Kogaku* (*Chem. Eng. Japan*), **17**, 176 (1953).

Perry, J. H., *Chemical Engineer's Handbook*, Fourth Edit., pp. 3-37, 70, 14-4, 14-6, McGraw-Hill, New York (1963).

Ralston, A., and H. S. Wilf, *Mathematical Methods for Digital Computers*, p. 110, Wiley, New York (1960).

Reid, R. C., and T. K. Sherwood, *The Properties of Gases and Liquids*, Second Edit., p. 559, McGraw-Hill, New York (1966).

Ross, L. D., "Performance of Trickle Bed Reactors," *Chem. Eng. Progr.*, **61**(10), 77 (1965).

Sadana, A., and J. R. Katzer, "Catalytic Oxidation of Phenol in Aqueous Solution over Copper Oxide," *Ind. Eng. Chem. Fundamentals*, **13**, 127 (1974).

Satterfield, C. N., *Mass Transfer in Heterog Catalysis*, p. 96, M.I.T. Press, Cambridge (1970).

———, and P. F. Way, "The Role of Liquid Phase in the Performance of a Trickle Bed Reactor," *AIChE J.*, **18**, 305 (1972).

Sedriks, W., and C. N. Kenney, "Partial Wetting in Trickle Bed Reactors—The Reduction of Crotonaldehyde over a Palladium Catalyst," *Chem. Eng. Sci.*, **28**, 559 (1973).

Sherwood, T. K., and F. A. L. Holloway, "Performance of Packed Towers—Liquid Film Data for Several Packings," *Trans. Am. Inst. Chem. Eng.*, **36**, 39 (1940).

Van Krevelen, D. W., and J. T. C. Krekels, "Rate of Dissolution of Solid Substances," *Rec. Trav. Chim.*, **67**, 512 (1948).

Washburn, E. W., (Ed.), *International Critical Tables*, First Edit., Vol. 5, p. 10, McGraw-Hill, New York (1929).

Weekman, V. W., and J. E. Myers, "Fluid-Flow Characteristics of Concurrent Gas-Liquid Flow in Packed Beds," *AIChE J.*, **10**, 951 (1964).

Manuscript received December 2, 1974; revision received February 3 and accepted February 14, 1975.